

# Toughened poly(butylene terephthalate) by blending with a metallocenic poly(ethylene–octene) copolymer

A. Aróstegui, M. Gaztelumendi, J. Nazábal\*

*Departamento de Ciencia y Tecnología de Polímeros and Instituto de Materiales Poliméricos 'POLYMAT', Facultad de Ciencias Químicas, UPV/EHU, P.O. Box 1072, 20080 San Sebastián, Spain*

Received 9 May 2001; received in revised form 19 June 2001; accepted 26 June 2001

## Abstract

New toughened poly(butylene terephthalate) (PBT) materials were obtained by melt blending with poly(ethylene–octene) copolymer (PEO) and maleic anhydride grafted PEO (gPEO) in a twin screw extruder followed by injection moulding at two injection speeds. The presence of either PEO or gPEO did not influence either the nature of the PBT phase or the crystallisation of PBT. Low injection speeds ( $7\text{ cm}^3/\text{s}$ ) and gPEO provided the best mechanical response. Increasing levels of maleic anhydride in gPEO led to a continuous overall decrease in the particle size, that was the most important when the particle size of the ungrafted PEO and that of the PEO at the minimum grafting level were compared. The decrease stopped at a grafting level between 1.14 and 1.80 due to the viscosity increase with the grafting level. Super-tough PBT based blends with impact strength more than twenty-fold that of PBT were obtained at PEO contents equal to or higher than 15%, and at decreasing PEO contents when the grafting level increased. The inter-particle distance ( $\tau$ ) is the parameter that controls toughness in these PBT/PEO blends. When the critical  $\tau$  ( $\tau_c$ ) measured in this work for PBT was compared with those obtained in other toughened blends at constant test conditions and rubber properties,  $\tau_c$  decreased as the modulus of elasticity of the matrix increased. When  $\tau_c$  of this work was compared with those obtained in other PBT/rubber blends, it depended on the modulus of elasticity of the dispersed phase, and it increased rather linearly as the PBT modulus to rubber modulus ratio increased. © 2001 Elsevier Science Ltd. All rights reserved.

*Keywords:* Poly(butylene terephthalate); Poly(ethylene–octene) copolymer; Super-toughness

## 1. Introduction

Poly(butylene terephthalate), PBT, is an important engineering thermoplastic due to its good combination of properties such as rigidity, solvent resistance and high rates of crystallisation that allow short cycle times in injection moulding [1,2], but its notched impact strength is very low. It can be improved by the incorporation of impact modifiers [3], such as acrylonitrile–butadiene–styrene (ABS) [4], emulsion made core-shell rubbers [5,6], acrylate–styrene–acrylonitrile [7] and butadiene-*co*-acrylonitrile [8]. The impact strength increases obtained are significant, but much higher increases have been achieved recently with the so-called super-tough PBTs, by means of blending with functionalised rubbers. Super-toughness is thought to be achieved because the carboxylic or hydroxyl end groups of PBT can react during melt blending with the functionalised rubber to produce grafted molecules which compati-

bilise the blend. As a consequence, PBT has been blended with modified rubbers such as ethylene–propylene–diene (EPDM) [9], ethylene–propylene (EPR) [10,11], ethylene [12], ABS [13–18] and styrene–(ethylene-*co*-butadiene)–styrene copolymer (SEBS) and ethylene olefin rubber [19]. The most common functional groups used for grafting these rubbers were maleic anhydride [20–23] and epoxy [9,12,20,22].

Variables such as the molecular weight and the crystallinity of the matrix, the rubber content and particle size, and the interface characteristics, have the most important influence on the level of toughening. Besides the theory that attributes the brittle–ductile transition to a competition between fracture stress and shear yielding stress [24], many studies have focused on the optimum particle size of the rubber as the main parameter that influences toughness, although it seems to depend on the rubber volume fraction [3,21,25–27]. Wu proposed a model where super-toughness in rubber toughened blends was achieved when the inter-particle distance ( $\tau$ ) between two neighbouring particles was below a critical value [28]. Later studies on  $\tau$  as the

\* Corresponding author. Tel.: +34-943-018-218; fax: +34-943-212-236.  
E-mail address: popnaetj@sq.ehu.es (J. Nazábal).

parameter that controls toughness have focused on polyamides [28–31], HDPE [32] and some engineering thermoplastics [19]. These  $\tau$  values have been proposed to be either characteristic of each matrix [28,31,32] depending on the strain rate [33,34], mode of deformation [31], temperature [19,29,31,35], plasticiser [36] and so on, or a function of additional parameters [19,30,37].

Poly(ethylene–octene) copolymer (PEO) is a new polyolefin elastomer developed using a metallocene catalyst by the Dow Chemical Co. PEO is characterized by a narrow molecular weight distribution and homogeneous octene distribution. Compared with conventional polyolefin elastomers, i.e. EPDM or EPR, PEO exhibits the advantage of thermoplastic processability. The elastomeric nature of PEO has allowed its use as an impact modifier for PP [38–41] and PE [32,39–41]. Maleinised PEO has been used for polyamides [42–46] and for an amorphous copolyester (PETG) [47]. Thus, PEO seems to be a possible suitable impact modifier for PBT.

PBT/PEO blends have not been studied, to our knowledge, up to now. For this reason, the purpose of this study is to examine the possibility of increasing the notched impact resistance of PBT using PEO grafted with maleic anhydride via melt extrusion. Firstly, preliminary work was carried out to test the possibility of toughness improvement, and to choose the best injection conditions. Subsequently, blends with PEO contents from 0 to 30% and with a grafting range from 0 to 1.80% were obtained by extrusion and subsequent injection moulding. They were characterized by differential scanning calorimetry (DSC), DMTA, scanning electron microscopy (SEM), contact angle measurements, Fourier transform infrared spectroscopy (FTIR) and viscosity measurements. The values of the tensile and impact properties as a function of the PEO content and grafting level indicated the best PEO content and grafting level, and the range of PEO content and grafting level at which maximum toughness is present in these blends. The  $\tau$  value obtained was used to discern whether  $\tau$  is a characteristic of each matrix or also depends on other parameters such as the modulus of elasticity of the rubber.

## 2. Experimental

### 2.1. Materials

The PBT used in this work was CRAFTIN S600F10 (DuPont) and the PEO rubber was ENGAGE EG 8200 (DuPont–Dow). The proportion of octene in the PEO was 24% by weight. The reactive monomer used for grafting was a commercial maleic anhydride (MA, 98% purity) and the peroxide initiator was dicumyl peroxide (DCP) (Aldrich). Both the PBT (4 h at 120°C) and the PEO (6 h at 60°C) were dried before processing in an air oven to avoid possible moisture-degradation reactions.

### 2.2. Grafting procedure and grafted rubber content

The grafting of PEO was carried out by mixing MA (from 0.5 to 5 wt%) with a constant DCP (0.05 wt%). Mixing was carried out in a Collin twin screw extruder–kneader (type ZK 25) of *L/D* ratio 24 and screw diameter of 25 mm. The temperature profile along the extruder was 50, 140, 155, 170, 170, and 175°C and the rotor speed was 70 rpm. The rod extrudate was cooled in water, and then pelletised. The pellets were placed in methanol for 48 h to remove free MA [48], and then dried at 60°C for 2–3 days.

The amount of grafted MA in the PEO was determined by titration [23,48–50]. The maleic anhydride grafted PEO (gPEO) was dissolved in toluene and when distilled water was added, three different phases appeared: an aqueous, a gel and an organic. The gPEO, in the organic phase, was titrated with 0.01 M KOH in ethanol. At least, three measurements were made for each reported value. The amount of gPEO is shown in Fig. 1 as a function of the added MA. As can be seen, the amount of gPEO increased with the amount of added MA up to 3 wt%. MA of 5 wt% did not change the grafting level significantly. PEO-0.32 indicates that the amount of grafted MA of the PEO is 0.32%.

### 2.3. Reactive blending and moulding procedures

Blending was carried out in the twin screw extruder–kneader used for the melt free radical grafting. PBT/PEO 90/10 and 85/15 and PBT/gPEO 90/10, 85/15 and 80/20 blends were processed at 250°C, whereas PBT/PEO 80/20 and 70/30 and PBT/gPEO 70/30 blends were processed at 225°C because of the low melt strength at 250°C. The rotor speed was 50 rpm. The rod extrudate was cooled in a water bath, and then pelletised.

Injection moulding was carried out in a Battenfeld BA230E reciprocating screw injection moulding machine to obtain tensile (ASTM D638, type IV, thickness 3.2 mm) and impact (ASTM D256, thickness 3.2 mm) specimens. The screw had a diameter of 18 mm and a *L/D* ratio of 17.8. Two different injection speeds (17 and 7 cm<sup>3</sup>/s)

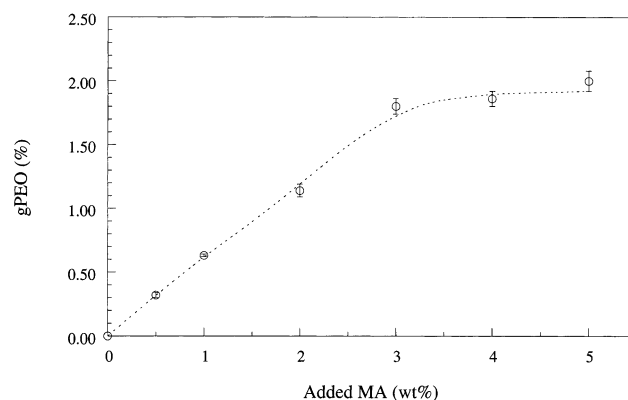


Fig. 1. The amount of grafted MA on PEO as a function of added MA.

were used. A high injection speed would avoid [1,2] premature freezing in the mould. The melt temperature was 250 and 260°C, respectively, at the high and low injection speeds. The injection pressure was 120 MPa, and the mould temperature was 60°C. However, for neat PEO, the melt temperature was 190°C, and the mould temperature 15°C.

The torque of PEO and gPEOs was measured by a Brabender Plasticorder, at 250°C and at 100 rpm (intermediate speed between that of the extruder and that of the injection machine). The operation was maintained for roughly 20 min until a constant torque was obtained.

#### 2.4. Solid state structure

The phase structure of the neat polymers and of the blends was studied by DSC using a Perkin–Elmer DSC-7 calorimeter and indium as reference. The samples were first heated from 10 up to 270°C at 20°C/min, then cooled at the same rate, and heated again. The crystallisation and melting temperatures and the enthalpies were determined from the maxima and the areas of the corresponding peaks, respectively. Dynamic mechanical analysis was performed on a Polymer Laboratories DMTA that provided the plots of the loss tangent ( $\tan \delta$ ) and the storage moduli ( $E'$ ) against temperature. The scans were carried out in bending mode at a constant heating rate of 2°C/min and a frequency of 1 Hz, from –130°C until the sample became too soft to be tested.

The possible reactions between PBT and gPEO were studied by FTIR, using a Nicolet 5 DXC spectrophotometer. The contact angle measurements were carried out on a CAM 100 goniometer (KSV) on injection moulded tensile bars, using water and ethylene glycol. The mean standard deviation of the measurements was 2–3° which gave rise to an error in the interfacial tension values of approximately 20%.

The surfaces of cryogenically fractured specimens were observed by SEM after gold coating. A Hitachi S-2700 electron microscope was used at an accelerating voltage of 15 kV. The particle size of the rubber was measured in representative zones of the cryogenically fractured impact specimens. The weight-average particle size ( $\bar{d}_w$ ) was calculated from a minimum of 200 particles as

$$\bar{d}_w = \frac{\sum n_i d_i^2}{\sum n_i d_i}$$

where  $n$  is the number of particles with size  $d$ .

#### 2.5. Mechanical properties

The tensile tests were carried out using an Instron 4301 tensile tester at a cross-head speed of 10 mm/min and at  $23 \pm 2^\circ\text{C}$ . The mechanical properties (Young's modulus,  $E$ ; tensile strength; and, ductility, measured as the break strain,  $\epsilon_b$ ) were determined from the load–displacement curves. The Young's modulus was determined by means

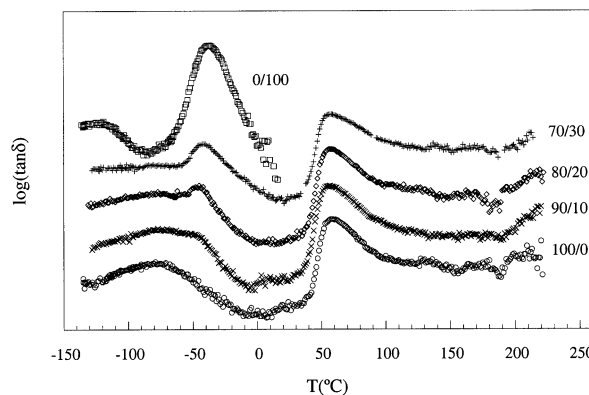


Fig. 2. DMTA  $\log(\tan \delta)$  versus temperature of PBT/PEO-0.63 blends. To aid clarity, the curves are shifted on the vertical axis.

of an extensometer. The elongation at break was determined from the crosshead travel rate assuming a gauge length of 64 mm. Izod impact tests were carried out on notched specimens using a CEAST 6548/000 pendulum. The notch (depth 2.54 mm and radius 0.25 mm) was machined after injection moulding. A minimum of five tensile specimens and ten impact specimens were tested for each reported value.

### 3. Results and discussion

#### 3.1. Phase structure

The phase structure of PBT/PEO blends was studied by DMTA. The DSC scans did not provide additional information on the  $T_g$  behaviour. For this reason, the only DMTA results which are shown in Fig. 2 will be discussed. The transitions of PEO did not significantly change with the grafting level; therefore, only the scans that correspond to PEO-0.63 are shown. As can be seen, the  $T_g$  and the secondary transition of the PBT in the blends remained constant at 58 and  $-77^\circ\text{C}$ , respectively. With respect to the glass transitions of the PEO, the secondary glass transition (at  $-121^\circ\text{C}$ ) could not be seen in the blends probably because of the low PEO content. The slight change of the  $T_g$  of the PEO in the blends was also seen in PP/PEO blends [39], and was probably due to the different processing conditions used.

The melting behaviour of the PBT/PEO blends was studied by DSC and the corresponding results of the first scan are shown in Fig. 3. As can be seen, no crystallisation exotherm was observed in spite of the fast cooling in the injection mould. The  $T_m$  ( $228^\circ\text{C}$ ) and the crystallinity (33%) of PBT were the same in the two scans and as is seen in Fig. 3, they remained constant with the PEO content. This agrees with previous results in other semicrystalline matrix/elastomer blends [38,40]. The constancy of the crystallinity level indicates that the elastomeric phase does not disturb the crystallisation process of PBT. As can also be seen in Fig. 3 when the 80/20-0.63 and 80/20-1.80 scans are

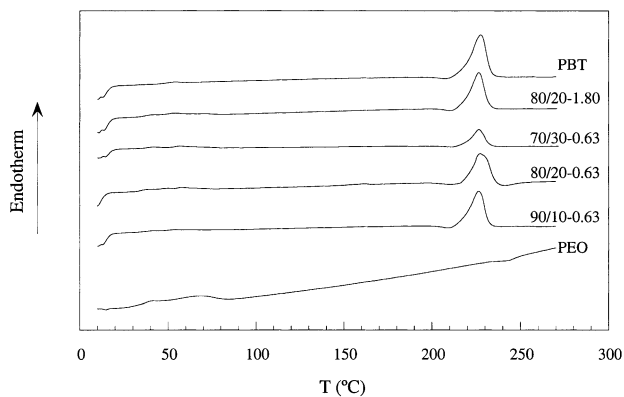


Fig. 3. First heating DSC heating scans of the pure PBT and PEO, and of the 90/10-0.63, 80/20-0.63, 70/30-0.63 and 80/20-1.80 blends. To aid clarity, the curves are shifted on the vertical axis.

compared, neither the  $T_m$  nor the crystallinity of PBT significantly changed with the grafting level of PEO.

### 3.2. Effects of the injection conditions

A preliminary study of the mechanical properties was first carried out on PEO-0 and PEO-1.14 to choose suitable injection conditions for the blends. After blending in the extruder, two injection speeds were used; the melt temperature was also changed slightly. The Young's modulus and the tensile strength of the blends were very similar, whatever the injection speed and the grafting level. Moreover, they decreased gradually at the two injection speeds when the PEO-0 or PEO-1.14 content increased due to the elastomeric nature of both PEOs [43,47,51].

The ductilities of PBT/PEO blends at the two grafting levels (0 and 1.14) and the two injection speeds are shown in Fig. 4. The ductility as well as the rest of the mechanical properties were plotted against both the weight and volume composition due to the different densities of PBT ( $1.31 \text{ g/cm}^3$ ) and PEO ( $0.87 \text{ g/cm}^3$ ). As can be seen, the ductility of

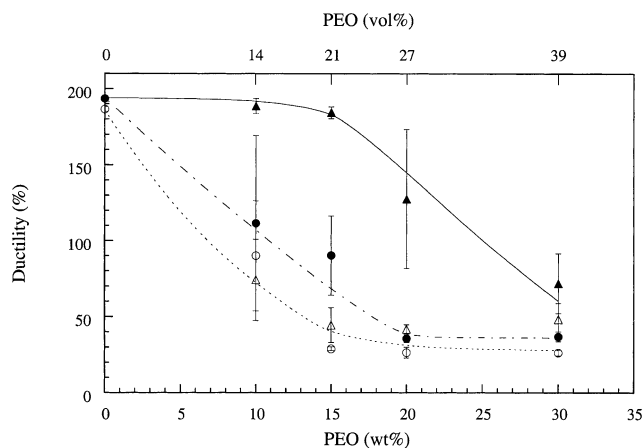


Fig. 4. The ductility of PBT/PEO blends as a function of PEO content at high (open symbols) and low (filled symbols) injection speed for 0 ( $\circ$ ,  $\Delta$ ) and 1.14 ( $\bullet$ ,  $\blacktriangle$ ) grafting levels.

the blends was higher at the low injection speed, whatever the PEO and grafting contents. The ductility decreased with the PEO content despite the rubber nature of PEO, indicating the incompatibility of the blend. The grafting (triangles) did not change the ductility of the blends at the high injection speed (open symbols), but at the low injection speed (filled symbols), the ductility clearly improved after grafting. This is a first indication of the fact that compatibilisation took place.

Fig. 5 shows the impact strength at both injection speeds and grafting levels. Most of the values corresponding to the blends with gPEO injected at high speed (open triangles) were divided and are plotted in Fig. 5 in two groups of clearly different impact strength. The plotted curve of the open triangles (line and point) takes into account the values of the two groups. As can be seen, the impact strength of the grafted blends (triangles) is clearly higher than that of the ungrafted ones (circles) indicating, as in the case of the ductility, compatibilisation. As can also be seen, the impact strength of the blends with unmodified PEO (circles) was the same at both injection speeds. However, the impact strength of PBT/PEO-1.14 blends at low injection speed, and some of the specimens at high injection speed showed impact strengths much higher than that of PBT (fifteen-fold typically). Therefore, super-toughness takes place in these blends and is more probable at low injection speeds.

The reason for the two different toughness values of the specimens at the high injection speed, which are plotted separately in Fig. 5 does not seem to be a brittle–ductile transition, because it takes place at very different PEO contents. Therefore, to find out the reason for this behaviour, the morphology of the two groups of specimens was compared. The size and shape of the PEO dispersed phase at both injection speeds were practically the same. However, in the group with low impact strength, the cryofractured surface at an angle of  $60^\circ$  from the perpendicular to the surface showed at low magnification a clear crack through the whole specimen, indicating that jetting took place. This

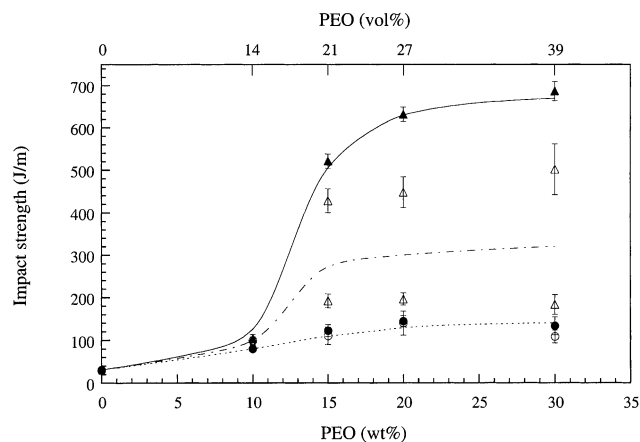


Fig. 5. The impact strength of PBT/PEO blends as a function of PEO content. Symbols as in Fig. 3.

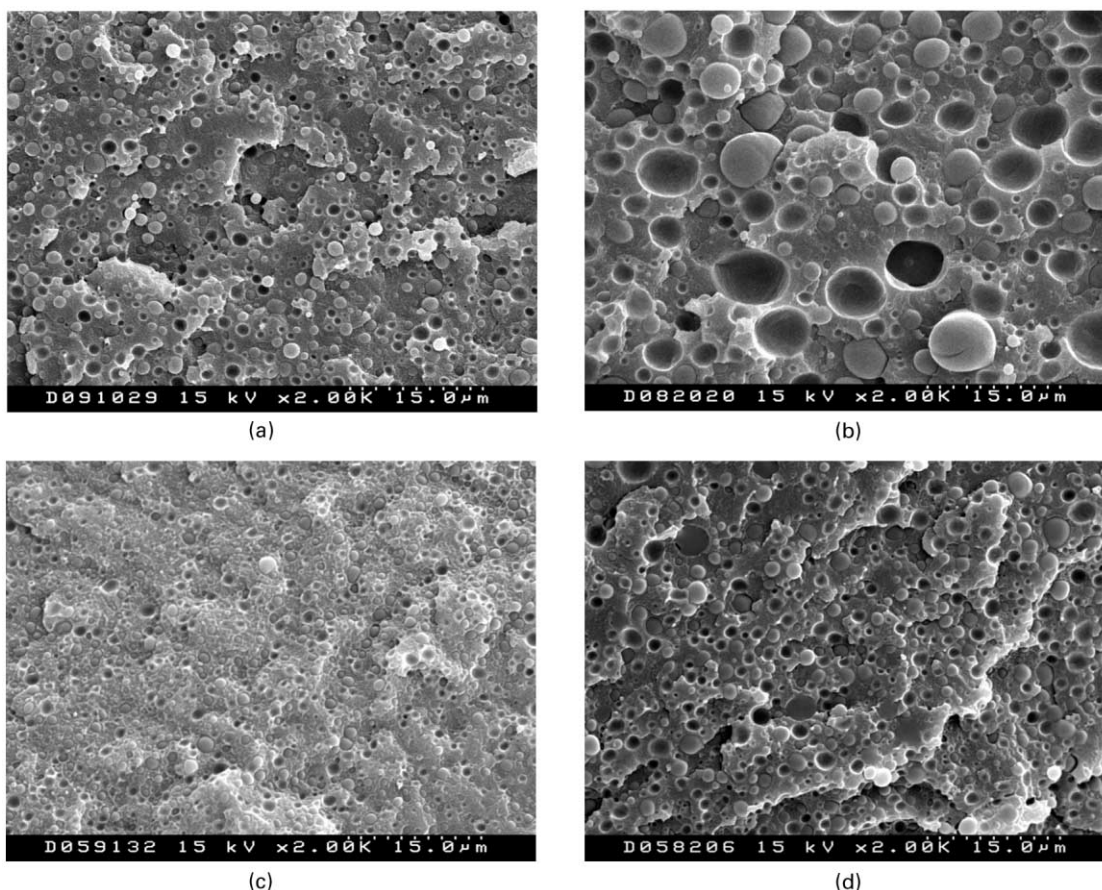


Fig. 6. The cryofractured surface of the inner zone of injection moulded impact specimens of PBT/PEO-0 90/10 (a) and 80/20 (b) blends, and of PBT/PEO-0.32 90/10 (c) and 80/20 (d) blends.

appeared sometimes at high injection speed, leading clearly to a lower impact strength, whatever the PEO content. Ductility was also lower at high injection speed. Therefore, a low injection speed ( $7 \text{ cm}^3/\text{s}$ ) was used in the following sections where the effects of the PEO content and of the grafting level on the structure and mechanical properties of the blends will be studied.

### 3.3. Morphology

The cryofractured surfaces of the injection moulded impact specimens were observed by SEM. A fine layer (about  $100\text{--}150 \mu\text{m}$ ) with elongated rubber particles also observed in PET/SEBS-g-MA blends [51,52] covered the specimens. Such a layer was not considered in the discussion of the morphology due to its low thickness and in consequence negligible influence on the mechanical properties. In the rest of the transverse section, the morphology was slightly different close to the exterior of the specimen and in the core. We will refer to these two different parts as the outside part and the inner part of the transverse section of the specimen.

The typical morphology of the inner part of the 90/10-0 and 80/20-0 blends is shown respectively in Fig. 6a,b. The

morphology of the same blends with PEO-0.32 is shown respectively in Fig. 6c,d. The morphology of the outside part whatever the PEO content was slightly finer than that of the inner part, and occupied roughly a third of the thickness of the specimen. This can be seen when the morphology of the inner part of the 80/20-0.32 blends of Fig. 6d is compared with that of the correspondent of the outside part

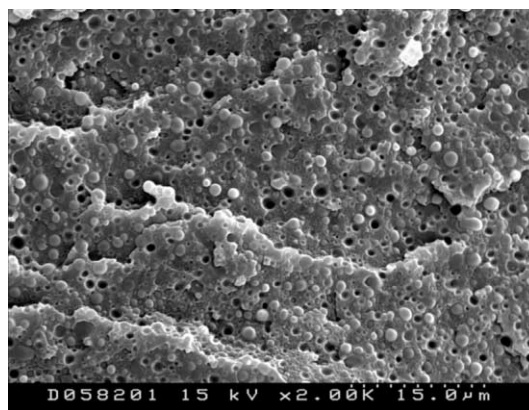


Fig. 7. The cryofractured surface of the outside zone of the injection moulded impact specimen of PBT/PEO-0.32 80/20 blend.

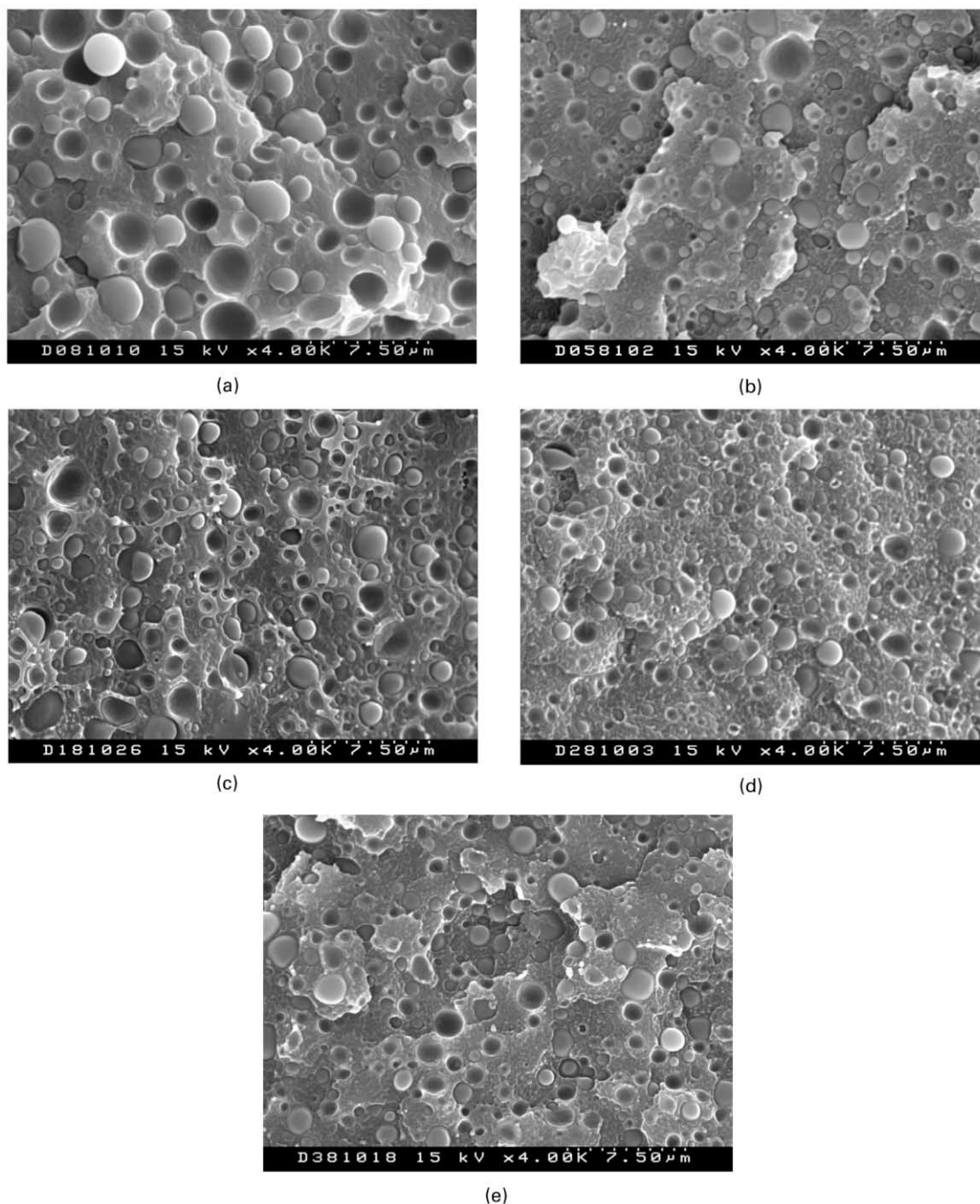


Fig. 8. The cryofractured surface of the inner zone of injection moulded impact specimens of PBT/PEO-0 (a), PBT/PEO-0.32 (b), PBT/PEO-0.63 (c), PBT/PEO-1.14 (d) and PBT/PEO-1.80 (e) 85/15 blends.

which is shown in Fig. 7. This was probably because cooling was faster in the outside part and, thus, the possibility of coalescence decreased. Moreover, the shear rate when the polymer fills the mould is much higher in the outside part of the specimen, which is close to the mould than in the inner part. This leads to easier coalescence in the inner part, and should lead to a larger dispersed particle size. The PEO blends grafted at levels other than 0.32 showed similar morphology changes when the PEO content changed. The

influence of the grafting level on the morphology will be commented later in the case of the 85/15 blend.

As can be seen in Fig. 6a,b, the increase in the particle size of uncompatibilised blends is higher than that which took place in PEO-0.32 blends (Fig. 6c,d). The smaller particle size of the blends with gPEO proves that the gPEO makes the dispersion easier and improves the compatibility of the blends. Similar behaviour was seen in other rubber toughened blends when compatibilised rubbers were used [42,43,48,51,52].

Table 1

The weight-average particle size ( $\bar{d}_w$ ) of PBT/PEO 85/15 blends in the outside part, the inner part, and the whole specimen (33% outside part, 67% inner part)

Grafting level (%)	$\bar{d}_w$ ( $\mu\text{m}$ )		
	Outside part	Inner part	Average
0	$1.25 \pm 0.13$	$1.68 \pm 0.24$	1.52
0.32	$0.86 \pm 0.09$	$1.24 \pm 0.19$	1.10
0.63	$0.78 \pm 0.09$	$0.96 \pm 0.15$	0.89
1.14	$0.73 \pm 0.09$	$0.83 \pm 0.10$	0.79
1.80	$0.86 \pm 0.09$	$1.15 \pm 0.19$	1.04

In order to investigate the reason for the improved compatibility of grafted blends, the interfacial tensions in both the ungrafted and grafted blends were measured by means of the contact angles between PBT and PEO-0, and also between PBT and gPEO. The interfacial tension between PBT and PEO-0 was 1.79 mN/m, meanwhile between PBT and gPEOs, whatever the grafting level, was roughly 0.25 mN/m. Although the interfacial tension does not apparently change with the grafting level it may change slightly, because the estimated error of the measurement was 20%. Therefore, the use of gPEO clearly decreased the interfacial tension, and as a consequence, the compatibility between PBT and PEO improved and the particle size decreased. The decrease in the interfacial tension could be due either to grafting reactions at the interphase, or to specific interactions between PBT and gPEO, or to both. The possibility of reactions was tested by FTIR, but no significant sign of reactions was observed. This indicates that, if chemical reactions took place, their extent was small.

As can also be seen in Fig. 6a,b, the adhesion level between PBT and PEO is poor. This is seen because the surfaces of both the particles and the holes are very clear and regular. Unexpectedly, in the case of Fig. 6c,d the adhesion level appears almost as poor as that of the ungrafted blends.

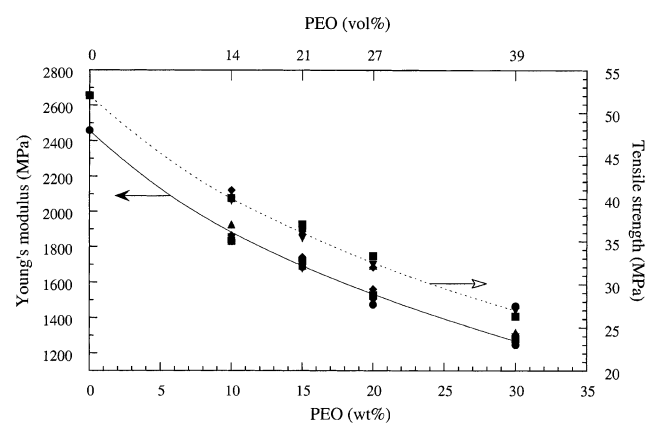


Fig. 9. The Young's modulus and the tensile strength as a function of PEO content at 0 (●), 0.32 (◆), 0.63 (▼), 1.14 (▲) and 1.80 (■) grafting levels.

The effects of the grafting level on the morphology of the blends will be studied in the case of the 85/15 blends. The blends with other PEO contents showed similar trends in morphology at different grafting levels. Fig. 8 shows the cryogenically fractured surfaces of the inner zone of impact specimens of 85/15 blends at 0 (a), 0.32 (b), 0.63 (c), 1.14 (d) and 1.80 (e) grafting levels. The correspondent weight-average particle size,  $\bar{d}_w$ , values are shown in Table 1 together with the calculated standard deviations. As can be seen in Table 1, the changes with the grafting content of the particle size in the inner and outside zones were similar. As can also be seen in Fig. 8 and Table 1, when the grafting level increased from PEO-0 to PEO-0.32,  $\bar{d}_w$  clearly decreased. Above 0.32%, the decrease was smaller, and finally  $\bar{d}_w$  increased.

The decrease in the rubber particle size when the grafting level increases is consequent with the increase in the interactions or grafting reactions at the interface [20,25,26,53,54]. However, the increase in  $\bar{d}_w$  observed in the 85/15-1.80 blend is unexpected. This is because more gPEO leads to an increase in the number of functional groups leading to a higher probability to interact and, as a consequence, to smaller interfacial tension. However, the viscosity of PEO may increase with grafting, hindering both the PEO particles deformation and their breaking into smaller particles into the predominantly PBT melt matrix. For this reason, the viscosity of PEO with different grafting levels was measured in a Brabender Plasticorder at 100 rpm (intermediate speed between that of the extruder and the injection machine) against time. The torque, and as a consequence the viscosity, increased with the grafting content, whatever the residence time in the plasticorder. Therefore, higher grafting levels led to a higher PEO viscosity and to an increasing particle size effect that will probably overcome the opposite effect of the increasing grafting level. In fact, the effect of the increasing grafting level decreasing the interfacial tension is usually less relevant when intermediate or large compatibiliser amounts are present.

### 3.4. Mechanical properties

Fig. 9 shows the Young's modulus and the tensile strength of PBT/PEO blends against the grafting level. As can be seen, when the PEO content increased, the modulus and the tensile strength decreased, due to the elastomeric nature of PEO [43,47,51]. The modulus and the tensile strength were very similar whatever the grafting level. So, as in other previous works [25,52,55] the improved compatibility did not have a significant effect on the low-strain tensile properties.

In the case of ductility, it decreased with the PEO-0 content despite the rubbery nature of PEO as was seen in Fig. 4. This indicated that the interactions in PBT/PEO-0 blends are very weak. However, as was also seen in Fig. 4, the presence of gPEO clearly increased the ductility of the

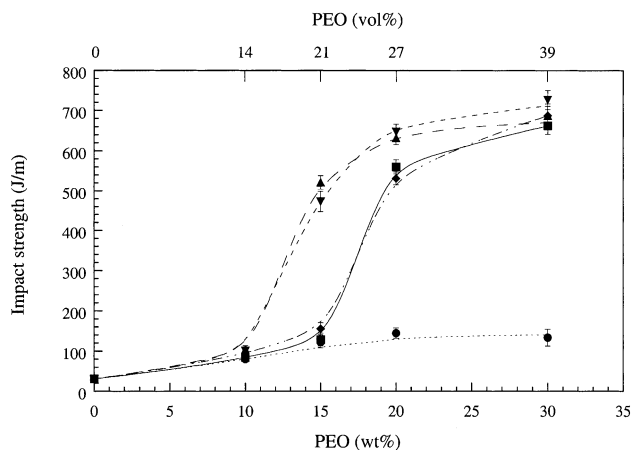


Fig. 10. The impact strength of PBT/PEO blends as a function of the PEO content at different grafting levels. Symbols as in Fig. 8.

blends, with ductility values that were almost identical to those of the pure PBT. This took place up to 15 wt% PEO mainly and whatever the grafting level. This indicates that grafting improved the compatibility in PBT/gPEO blends and that additional grafting has a comparatively minor influence on ductility.

Fig. 10 shows the impact strength of PBT/PEO blends at different grafting levels as a function of the PEO content. As can be seen, the impact strength of PBT/PEO-0 blends improved from roughly 30 J/m in the 100/0-0 blend to 135 J/m in the 70/30-0 blend. The additional impact strength due to grafting was slight at 10 wt% gPEO. The impact strength then increased very strongly as the PEO-0.32 and PEO-1.14 contents approached 20 wt%, and the PEO-0.63 and PEO-1.80 contents of the blend approached 15 wt%. Finally, an increase in gPEO up to 30 wt% content led to smaller increases that were independent of the grafting level and that increased the impact strength up to roughly 700 J/m. Even more, the super-tough PBT blends did not fully break under the notched Izod impact test, because roughly 25% of the specimen (2.5 mm thick) in the opposite side of the notch stayed unbroken. Therefore, the impact strength was typical of super-tough blends, because it was more than twenty-fold that of pure PBT and about six-fold that of the corresponding blends with ungrafted PEO. The large impact strength enhancement obtained for grafted blends, as stated before in the case of the ductility, was a consequence of the finer dispersion of PBT/gPEO blends.

The impact strength improvement obtained can be compared with that obtained in epoxidised PBT/EPDM [9] blends, because in both studies super-tough PBTs were obtained as the rubber content approached 15 wt% giving impact strengths more than twenty-fold that of pure PBT. Similar super-toughness was found in PBT with a 20 wt% core-shell impact modifier and PC as dispersing agent [6]

It must be noted that the observed impact strength increases when grafting took place under rather poor adhesion conditions as was commented in Fig. 6c,d and

can be also seen in Figs. 7 and 8b–e. This indicates that relevant adhesion is not a condition for super-toughness in rubber toughened blends, and that only low or even poor adhesion levels, almost not detectable by SEM, are enough for super-toughness is attained.

All PBT/PEO blends showed stress-whitening after fracture. The width of the stress-whitening zone changed with the PEO content and the grafting level. Thus, in the blends with low impact strength the stress-whitening zone was only around the notch, meanwhile super-tough PBT blends showed an intense stress-whitening along the whole fracture surface.

The proposition based on a minimum critical particle diameter of the rubber ( $d_c$ ) [3,21,25–27] to predict the large impact strength increases in rubber toughened blends was tested comparing the mean particle size of the 90/10-1.80 and the 85/15-1.14 blends, that were respectively brittle and super-tough. The particle size of the 85/15-1.14 blend (0.79  $\mu\text{m}$ ) was very similar to that measured in the 90/10-1.80 blend (0.81  $\mu\text{m}$ ). As a consequence, the proposition based on a minimum particle diameter of the rubber is only valid at a given volume fraction.

Wu [28] proposed that the impact strength increase should occur when the inter-particle distance ( $\tau$ ) between two neighbouring particles is below a critical value ( $\tau_c$ ).  $\tau$  is defined as

$$\tau = \bar{d}_w \left[ \left( \frac{\pi}{6\phi} \right)^{1/3} - 1 \right] \quad (1)$$

where  $\bar{d}_w$  is the weight-average particle size, and  $\phi$  is the volume fraction of rubber.  $\tau_c$  is independent of the particle size and the rubber volume fraction, and is characteristic of a given matrix. It has even been seen [56] that rigid dispersed phases could also lead to increased toughness. Subsequent works showed that  $\tau_c$  also depended on the test temperature [19,29,31,35], plasticisers [36], the strain rate [31,32,34] and the mode of deformation [31], the crystallinity of the matrix [19], and the type [30] or modulus [19] of rubber. To find out whether  $\tau_c$  limits the impact

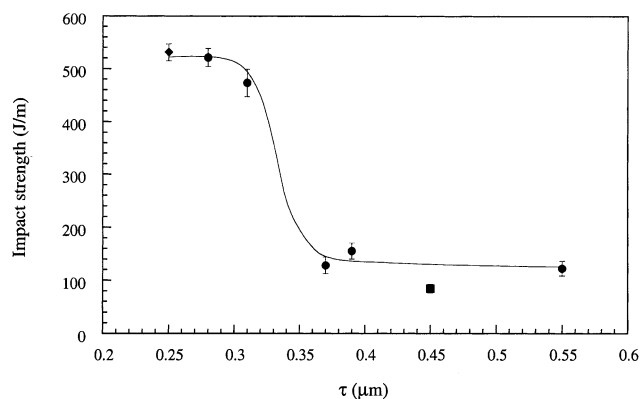


Fig. 11. The impact strength as a function of the inter-particle distance for 85/15 (●) at different grafting levels, 90/10-1.80 (■) and 80/20-0.32 (◆).



Table 2

The critical inter-particle distance ( $\tau_c$ ) of PBT/PEO blends and different rubber toughened matrices, and the modulus of elasticity of the matrices

Matrix	Dispersed phase	References	$E_m$ (MPa)	$\tau_c$ ( $\mu\text{m}$ )
HDPE	EPDM, PEO	[33]	756	0.6
PETG	Rubber	[49]	1900	0.44
PBT	Ethylene-olefin	[48]	2750	0.40
PBT	PEO	This work	2450	0.33
Nylon 6	EPDM	[46]	2500	0.31
Nylon 6,6	Rubber	[38]	2800	0.30
PPS	Rubber	[48]	3800	0.2
POM	Rubber	[48]	2400	0.18
PBT	SEBS	[48]	2750	0.16
Nylon 6	Silica	[50]	2500	0.065

strength behaviour of these blends, and based on the  $\bar{d}_w$  values of Table 1 and Eq. (1), the  $\tau$  of the 85/15 blends with different grafting levels were measured and the values (filled circles) plotted in Fig. 11 against the impact strength. As can be seen, a sharp increase in impact strength took place when  $\tau$  decreased below roughly  $0.33 \mu\text{m}$ . This  $\tau$  is considered as  $\tau_c$  for the PBT in this work. This  $\tau_c$  is independent of the rubber volume fraction. This is because the calculated  $\tau$  of the 90/10-1.80 blend ( $0.45 \mu\text{m}$ ) was above  $\tau_c$ , in agreement with its relatively low toughness. That of the 80/20-0.32 blend ( $0.25 \mu\text{m}$ ) was below  $\tau_c$ , in agreement with its super-tough nature and Wu's model.

If we compare the  $\tau_c$  of this work with those of other matrices, the  $\tau_c$  of PBT of this work is similar to that observed in other rubber-toughened matrices of similar modulus; that of HDPE of smaller modulus is higher than that of this work, and that of PPS of higher modulus is smaller. For this reason, in Table 2 the  $\tau_c$  of different rubber toughened matrices are collected against the modulus of the matrix, and the nature of the dispersed phase when available. As can be seen, among the blends of the upper part of Table 2 the matrices with  $\tau_c$  between  $0.30$  and  $0.40 \mu\text{m}$  all have similar modulus of elasticity. The matrix with low modulus shows clearly higher  $\tau_c$  and the stiffest PPS matrix shows the lowest  $\tau_c$ . Moreover, in a study [57] on PBT/EPDM blends, when the modulus of the rubber was increased by irradiation, the brittle-tough transition took place at an increased rubber volume fraction (and as a consequence,  $\tau_c$ ) decreased. This data indicates that stiffer the matrix is, lower  $\tau_c$  is. However, there are exceptions which are reported at the bottom of Table 2. The high crystalline nature of POM and the special nature (mineral) of the filler of Ref. [56] may account for the observed behaviour. Moreover, an additional influence [19] of the modulus of the dispersed phase on  $\tau_c$  is not taken into account in Table 2. This will be discussed in the next paragraph.

The  $\tau_c$  obtained for PBT in this work ( $0.33 \mu\text{m}$ ) is between those obtained [19] in PBT/SEBS blends ( $\tau_c = 0.16 \mu\text{m}$ ) and PBT/ethylene olefin rubber blends ( $\tau_c = 0.40 \mu\text{m}$ ). This difference was attributed to the modulus of the dispersed rubber. The results of this work agree with this

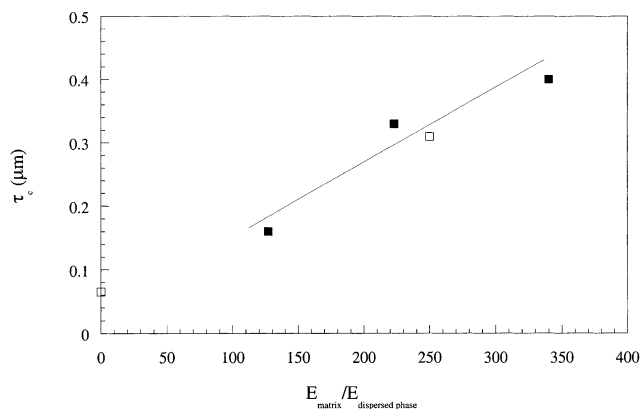


Fig. 12.  $\tau_c$  as a function of the  $E_m/E_d$  relation for PBT/PEO blends and nylon toughened blends.

supposition, because the modulus of elasticity of PEO (11 MPa) is also between the moduli of the two rubbers of Ref. [19] (22 MPa for SEBS and 8 MPa for the ethylene-olefin rubber). Therefore,  $\tau_c$  appears to depend on the nature of the dispersed phase. This is because the stress concentrations, which are the starting point of the toughness increase, will be higher [30] as the modulus difference between the matrix and the dispersed ( $E_m/E_d$ ) phase increases. To test the possibility of a dependence of  $\tau_c$  on the  $E_m/E_d$  relation, the  $\tau_c$  values of the PBT/rubber blends of Table 2 (filled symbols) were plotted against the  $E_m/E_d$  relation in Fig. 12. As can be seen, the  $\tau_c$ - $E_m/E_d$  relation of this work is just in the middle between those of PBT/SEBS and PBT/ethylene-olefin rubbers [19]. The  $\tau_c$  of the two Nylon 6 blends of Table 2 are also plotted in Fig. 11 as open squares taking 10 MPa for the modulus of EPDM and a very high value for the modulus of silica compared to that of PBT. In the case of Nylon 6,  $\tau_c$  also increases as the modulus of elasticity of the dispersed phase decreases. Thus, the dependence of  $\tau_c$  on the modulus of the dispersed rubber is confirmed. Furthermore, a linear relation between  $E_m/E_d$  and  $\tau_c$  is suggested by the plot of Fig. 12.

#### 4. Conclusions

Neither the presence of PEO nor the grafting level influenced the crystallinity of PBT or the phase nature of the two amorphous phases of the PBT/PEO blends. A low injection speed was suitable in the blends, as it provided higher ductility and impact strength and less processing related defects. The decrease in the interfacial tension in the blends, observed by contact angle measurements, led to a decrease in the dispersed particle size, that was most significant in ungrafted blends. The observed particle size increase at the highest grafting level was attributed to the increased melt viscosity of PEO with grafting.

Super-toughness and clear ductility improvements were observed when the grafting level of the gPEO was only

roughly 1% and adhesion in the interphase poor. The impact strength increase (typically ten-fold that of the blends with ungrafted PEO) appeared with a minimum of 15 wt% PEO and 0.63% gPEO. Higher PEO or grafting content led to additional slight asymptotic increases.

The inter-particle distance ( $\tau$ ) appears as the parameter that controls toughness in these PBT/PEO blends. At constant test parameters and leaving out the properties of the rubber, it generally decreases when the modulus of elasticity of the matrix increases. Moreover, when the  $\tau_c$  value of the PBT of this work (0.33  $\mu\text{m}$ ) was compared with those of other PBT/rubber blends, a fairly linear dependence of  $\tau_c$  on the relation between the modulus of the matrix and that of the rubbery dispersed phase was seen.

### Acknowledgements

The financial support of the University of the Basque Country (Project No. G46/98) is gratefully acknowledged. A. Aróstegui thanks the Basque Government for the award of a grant for the development of this work.

### References

- [1] Mark HF, Bikales NM, Overberger CG, Menges G, Kroschwitz JJ. Encyclopedia of polymer science and engineering, vol. 12. New York: Wiley, 1986.
- [2] Van Berkel RWM, Van Hartigsveldt EAA, Van der Sluijs CL. In: Olabisi O, editor. Handbook of thermoplastic. New York: Marcel Dekker, 1997 (Chapter 20).
- [3] Gaymans RJ. In: Paul DR, Bucknall CB, editors. Polymer blends, vol. 2. New York: Wiley, 2000 (Chapter 25).
- [4] Hage E, Hale W, Keskkula H, Paul DR. Polymer 1997;38(13):3237–50.
- [5] Mohd Ishak ZA, Ishiaku US, Karger-Kocsis J. J Appl Polym Sci 1999;74:2470–81.
- [6] Brady AJ, Keskkula H, Paul DR. Polymer 1994;35(17):3665–72.
- [7] Benson CM, Burford RP. J Mater Sci 1995;30:573–82.
- [8] Hourston DJ, Lane S, Zhang HX. Polymer 1995;36(15):3051–4.
- [9] Wang HX, Zhang HX, Wang ZG, Jiang BZ. Polymer 1997;38(7):1569–72.
- [10] Cecere A, Greco R, Ragosta G, Scarinzi G, Tagliatalata A. Polymer 1990;31:1239–44.
- [11] Vongpanish P, Bhowmick AK, Inoue T. Plast Rubber Compos Process Appl 1994;21(2):109–13.
- [12] Takashi A, Angola JC, Hiromu S, Takashi I, Yasushi N. Polymer 1999;40:3657–63.
- [13] Hale W, Keskkula H, Paul DR. Polymer 1999;40:365–77.
- [14] Hale W, Keskkula H, Paul DR. Polymer 1999;40:3353–65.
- [15] Hale W, Lee JH, Keskkula H, Paul DR. Polymer 1999;40:3621–9.
- [16] Hale W, Keskkula H, Paul DR. Polymer 1999;40:3665–76.
- [17] Hale WR, Pessan LA, Keskkula H, Paul DR. Polymer 1999;40:4237–50.
- [18] Lee PC, Kuo WF, Chang FC. Polymer 1994;35(26):5641–50.
- [19] Kanai H, Sullivan V, Auerbach A. J Appl Polym Sci 1994;53:529–41.
- [20] Majumdar B, Paul DR. In: Paul DR, Bucknall CB, editors. Polymer blends, vol. 1. New York: Wiley, 2000 (Chapter 17).
- [21] Keskkula H, Paul DR. In: Collyer AA, editor. Rubber toughened engineering plastics. London: Chapman and Hall, 1994 (Chapter 5).
- [22] Datta S, Loshe DJ. Polymeric compatibilizers. Munich: Hanser, 1996.
- [23] Grigoryeva OP, Karger-Kocsis J. Eur Polym J 2000;36:1419–29.
- [24] Ward IM. Mechanical properties of solid polymers. 2nd ed. New York: Wiley, 1983 (Chapter 12).
- [25] Oshinski AJ, Keskkula H, Paul DR. Polymer 1992;33(2):268–83.
- [26] Oshinski AJ, Keskkula H, Paul DR. Polymer 1992;33(2):284–93.
- [27] Bucknall CB. In: Paul DR, Bucknall CB, editors. Polymer blends, vol. 2. New York: Wiley, 2000 (Chapter 22).
- [28] Wu S. Polymer 1985;26:1855–63.
- [29] Borggreve RJM, Gaymans RJ, Schuijjer J, Ingen Housz JF. Polymer 1987;28:1489–96.
- [30] Borggreve RJM, Gaymans RJ, Schuijjer J. Polymer 1989;30:71–7.
- [31] Wu S. J Appl Polym Sci 1988;35:549–61.
- [32] Bartczak Z, Argon AS, Cohen RE, Weinberg M. Polymer 1999;40:2331–46.
- [33] Dijkstra K, ter Laak J, Gaymans RJ. Polymer 1994;35:315–22.
- [34] Jiang W, Tjong SC, Li RKY. Polymer 2000;41:3479–82.
- [35] Jiang W, Liu CH, Wang ZG, An LJ, Liang HJ, Jiang BZ, Wang XH, Zhang HX. Polymer 1998;39:3285–8.
- [36] Gaymans RJ, Borggreve RJM, Spoelstra AB. J Appl Polym Sci 1989;37:479–86.
- [37] van der Sanden MCM, de Kork JMM, Meijer MEH. Polymer 1994;35:2995–3004.
- [38] Da Silva ALN, Rocha MCG, Coutinho FMB, Bretas R, Scuracchio C. J Appl Polym Sci 2000;75:692–704.
- [39] Rana D, Lee CH, Cho K, Lee BH, Choe S. J Appl Polym Sci 1998;69:2441–50.
- [40] Paul S, Kale DD. J Appl Polym Sci 2000;76:1480–4.
- [41] Kwag H, Rana D, Cho K, Rhee J, Woo T, Lee BH, Choe S. Polym Engng Sci 2000;40:1672–81.
- [42] Chen H, Yang B, Zhang H. J Appl Polym Sci 2000;77:928–33.
- [43] Yu ZZ, Ou YC, Hu GH. J Appl Polym Sci 1998;69:1711–8.
- [44] Yu ZZ, Ou YC, Qi ZN, Hu GH. J Polym Sci B: Polym Phys 1998;36:1987–94.
- [45] Yu ZZ, Lei M, Ou YC, Hu GH. J Polym Sci B: Polym Phys 1999;37:2664–72.
- [46] Yu ZZ, Ke YC, Ou YC, Hu GH. J Appl Polym Sci 2000;76:1285–95.
- [47] Yu ZZ, Lei M, Ou YC, Yang G, Hu GH. J Polym Sci B: Polym Phys 2000;38:2801–9.
- [48] Seo Y, Hwang SS, Kim KU, Lee J, Hong SI. Polymer 1993;34:1667–76.
- [49] Oostenbrik AJ, Gaymans RJ. Polymer 1992;33(14):3086–8.
- [50] Sánchez-Solis A, Estrada MR, Cruz J, Manero O. Polym Engng Sci 2000;40(5):1216–25.
- [51] Tanrattanakul V, Hiltner A, Baer E, Perkins WG, Massey FL, Moet A. Polymer 1997;38(9):2191–200.
- [52] Tanrattanakul V, Hiltner A, Baer E, Perkins WG, Massey FL, Moet A. Polymer 1997;38(16):4117–25.
- [53] Oshinski AJ, Keskkula H, Paul DR. J Appl Polym Sci 1996;61:623–40.
- [54] Wu CJ, Kuo JF, Chen CY, Woo E. J Appl Polym Sci 1994;52:1695–706.
- [55] Moffet AJ, Dekkers MEJ. Polym Engng Sci 1992;32(1):1–5.
- [56] Ou Y, Yang F, Yu ZZ. J Polym Sci B: Polym Phys 1998;36:789–95.
- [57] Jiang W, Wang ZG, Liu HC, Liang HJ, Jiang BZ, Wang XH, Zhang HX. Polymer 1997;38:4275–7.